Proceedings of the 4th ITB Graduate School Conference
Innovation and Discovery for Sustainability
July 6, 2023

Synthesis and Characterization of Zeolite A-Calcium Carbonate for Carbon Capture

Muhammad Nauval Farras Russamsi[1,*], Triati Dewi Kencana Wungu[1,2] & Suprijadi[1,2]

[1]Nanotechnology Graduate Program, Institut Teknologi Bandung, Jalan Ganesa 10, Bandung 40132, Indonesia
[2]Physics Department, Institut Teknologi Bandung, Jalan Ganesa 10, Bandung 40132, Indonesia
[*]Email: 28721304@mahasiswa.itb.ac.id

Abstract. Carbon capture by solid adsorbents is one of the most promising ways to implement carbon capture. Zeolites, a class of aluminosilicate minerals with a honeycomb-like framework structure, has excellent carbon dioxide adsorption characteristics, attributed to its microporous nature. However, challenges remain to improve its adsorption characteristics, mainly related to its kinetics and selectivity. In this paper, zeolite A was treated with NaOH (zeolite-NaOH) and intercalated with calcium carbonate ($CaCO_3$) (zeolite-$CaCO_3$). The resultant material was then characterized by its morphology, crystallography, and its CO_2 adsorption characteristics. The results showed that treatment with NaOH did not change the morphology and crystallography of zeolite A, while intercalation with $CaCO_3$ showed that $CaCO_3$ formed nanoflowers in the surface of zeolite A and $CaCO_3$ exist in zeolite-$CaCO_3$ in both amorphous and crystalline form, co-existing with $Ca(OH)_2$ and CaO. Adsorption characteristics measured using thermogravimetric methods showed that zeolite-$CaCO_3$ had superior adsorption capacity, selectivity, and kinetics compared to zeolite A and zeolite-NaOH, especially by accounting for zeolite mass only in zeolite-$CaCO_3$.

Keywords: *adsorption; calcium carbonate; carbon capture; kinetics; selectivity; zeolite.*

1 Introduction

Carbon capture encompasses a range of techniques utilized to eliminate carbon dioxide either directly from the atmosphere or from its sources, predominantly flue gases produced through combustion. The Intergovernmental Panel on Climate Change [1] recognizes carbon capture as a crucial element in the efforts to mitigate climate change. Many challenges have been identified to apply carbon capture in a massive scale, the most pressing of them (as identified by Bajpai *et al.* [2]) are the energy and cost of implementation. Carbon capture by solid adsorbents is identified as one of the most promising methods. Raganati *et al.* [3] write that compared to all possible alternatives, capture by solid adsorbents had the greatest energy savings and is relatively easy to retrofit to existing industrial plants. Furthermore, Younas *et al.* [4] adds that solid adsorbents are easy to handle and do not cause corrosion problems.

As a result, many adsorbents have been developed to meet this demand, and one of the more promising ones is zeolite. Zeolites are aluminosilicate mineral compounds that possess a three-dimensional framework structure resembling a honeycomb. Zeolites are porous materials which commonly had microporous pore sizes (pore diameter < 2 nm), which is useful to capture, hold, and release compounds at molecular level. This ability means zeolites are classified as a molecular sieve. As carbon capture adsorbent, zeolites are one of the most promising materials due to its high adsorption capacity (Raganati *et al.* [3]).

Many variations of zeolite structures have been identified, some of them occurred naturally while others are synthetized. One variation is called zeolite A, also called LTA (Linde Type A) or NaA. Zeolite A is a type of synthetic zeolite with the chemical formula $[Na_{12}(H_2O)_{27}]_8[Al_{12}Si_{12}O_{48}]_8$. Each zeolite A framework consists of eight sodalite units ('cages') connected by four membered rings (D4R), forming a space (called α-cage) in the middle. The framework of zeolite A is depicted in Figure 1.

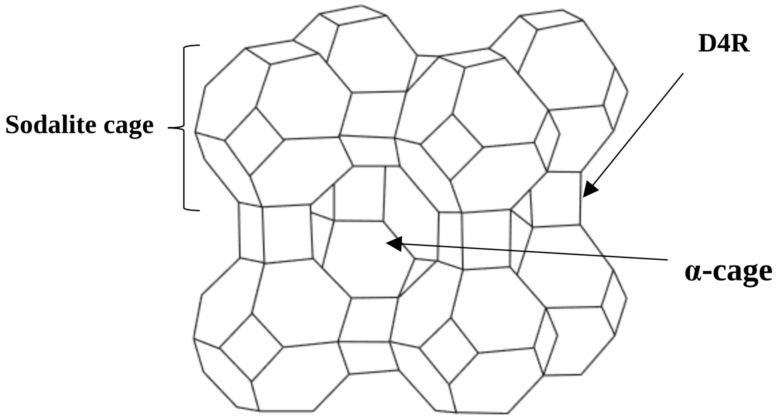

Figure 1 Zeolite A (Lutz [5])

Compared to other kinds of zeolites, zeolite A is preferred for carbon capture activities. Indira *et al.* [6] identified the advantages of zeolite A as having more affinity and being more selective towards CO_2 compared to N_2 and H_2. This is mainly due to its alkalinity caused by its low Al/Si ratio (CO_2 is a Lewis acid, so a more alkaline substance will have greater affinity towards it). However, zeolite A still has challenges in its adsorption kinetics. Thermogravimetric measurement done in this paper and by Cheung *et al.* [7] shows that zeolite A is quite slow to adsorb CO_2.

To tackle those problems, zeolite A could be further treated. Zeolites are often treated by acids, bases, or heated/calcined (Indira *et al.* [6]) in order to improve their characteristics. In this paper, zeolite A is activated by treating it with NaOH and further intercalating it with $CaCO_3$. NaOH was chosen in order to enhance the alkalinity of zeolite A, which in theory should improve the affinity of the adsorbent towards CO_2. Calcium carbonate is chosen due to its ability to activate adsorbents. While the use of calcium carbonate in activating zeolites for CO_2 adsorption is relatively novel, $CaCO_3$ has been studied as activating agent for carbon based adsorbers. For example, hierarchical porous carbon was combined with calcium carbonate for carbon capture adsorption by Gao *et al.* [8] and activated carbon was combined with $CaCO_3$ and $Ca(OH)_2$ for H_2S, CO_2, and NH_3 removal by Areerob *et al.* [9].

2 Materials and Methods

Three samples are characterized in this paper (zeolite A, zeolite A with NaOH, and zeolite A with $CaCO_3$). The samples will be referred to as zeolite A, zeolite-NaOH, and zeolite-$CaCO_3$, respectively. First, zeolite A was obtained from Sigma-Aldrich. To prepare zeolite-NaOH, zeolite A was first hydrated by stirring it in deionized water for 15 minutes, then treated using NaOH (1 M NaOH per 10 g of zeolite A) for 30 minutes at 80°C, then washed using deionized water until the pH is relatively neutral (7~8). Preparation of zeolite-$CaCO_3$ follows methods developed by Khine *et al.* for the synthesis of $CaCO_3$ [10]. 8.88 gr zeolite A was first hydrated, then stirred with 1 M $CaCl_2$ (8.88 gr in 80 ml deionized water) for 40 minutes. The mixture was then reacted with 3 M NaOH (9.6 gr in 80 ml) and further stirred for 30 minutes at 80°C, which causes the precipitation of $Ca(OH)_2$. The reaction between $CaCl_2$ and NaOH also results in the formation of NaCl. Using the quantities supplied, 8.6 gr of aqueous NaCl and 6.8 gr of $Ca(OH)_2$ solid were respectively formed. The resultant mixture was then washed repeatedly using deionized water to remove NaCl. The resultant solid, called zeolite-$Ca(OH)_2$, had a 1:0.77 mass proportion between zeolite A and $Ca(OH)_2$. It was then dried overnight and calcined at 650°C for 1 h in N_2 atmosphere. There are methods of synthetizing $CaCO_3$ from $Ca(OH)_2$ that do not involve calcination, such as reacting it with sodium carbonate. However, this method is chosen due to the theoretical advantage in activating zeolite by calcining it. Calcination will result in the formation of zeolite-CaO which after exposure to air, changes to zeolite-$CaCO_3$.

The samples are characterized for their morphology using SEM, crystallography using XRD, and its thermogravimetry to obtain its adsorption characteristics by using TG/DTA.

The adsorption characteristics of the materials is obtained using thermogravimetric methods developed by Chen and Lu [11]. The typical thermogravimetric plot resulting from following these methods are depicted in Figure 2. There are three steps, marked with A, B, and C, respectively. In step A, a small amount was loaded into the thermogravimetric machine, then heated to 150°C in a N_2 atmosphere for 40 min. This is done mainly to remove moisture and other impurities. After that, the temperature was lowered to 30°C in a 10°C/min temperature step, and the gas was switched to CO_2. This condition, also called step B, was held for 1 h. Step C was then conducted, with the gas switched back to N_2 and the temperature was raised back to 150°C for 40 min to desorb the CO_2 and obtain the complete adsorption-desorption characteristics of the material.

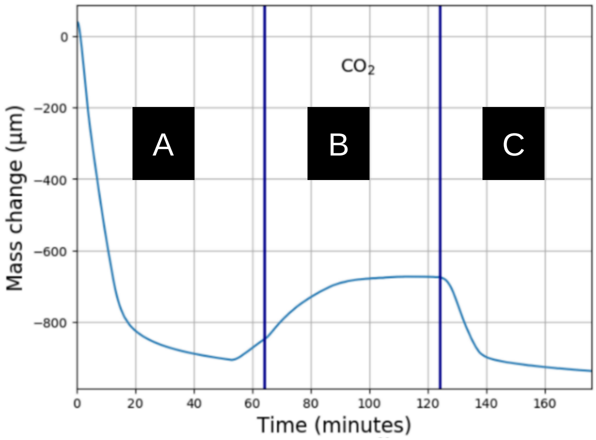

Figure 2 Thermogravimetric plot result of the method described by Chen and Lu [11].

The obtained thermogravimetric plot was subjected to three measurements. First, the adsorption capacity (C_{CO_2}) of the material was determined by calculating the difference between the mass at the beginning of step B and at the end of it, demarcated by a dark blue vertical line at the 64th minute (beginning) and 124th minute (end). Second, the adsorption kinetics (v) were evaluated by determining the gradient of the thermogravimetric plot during the initial 10 minutes of step B. The 10-minute duration was selected owing to the relatively linear nature of the plot across all samples analyzed. Third, the N_2 adsorption (C_{N_2}) of the materials was examined. It should be noted that the materials were not supposed to adsorb

N_2, however all samples evaluated demonstrated an increase in mass prior to switching to CO_2, indicating just that. The N_2 adsorption was measured by comparing the minimum mass during step A with the mass immediately preceding the onset of step B. It should be noted that minimum in this context has the meaning of 'the lowest point of the thermogravimetric curve'.

3 Results and Discussion

3.1 Morphology

The morphology of zeolite A, zeolite-NaOH, and zeolite-$CaCO_3$ taken by SEM was given in Figure 3. It is observed that zeolite A exhibits a cuboid morphology, with each one having a size of approximately 3-7 μm. There is no significant morphological changes in zeolite-NaOH compared to zeolite A, while SEM images of zeolite-$CaCO_3$ indicate the formation of calcium agglomerates in the surface of zeolite, which is otherwise relatively unchanged. These agglomerates formed a structure called nanoflowers by Thakur *et al.* [12]. Due to the reactions involved, these nanoflowers are predicted to consist of either CaO or $CaCO_3$. The composition of them will be discussed in the crystallography section.

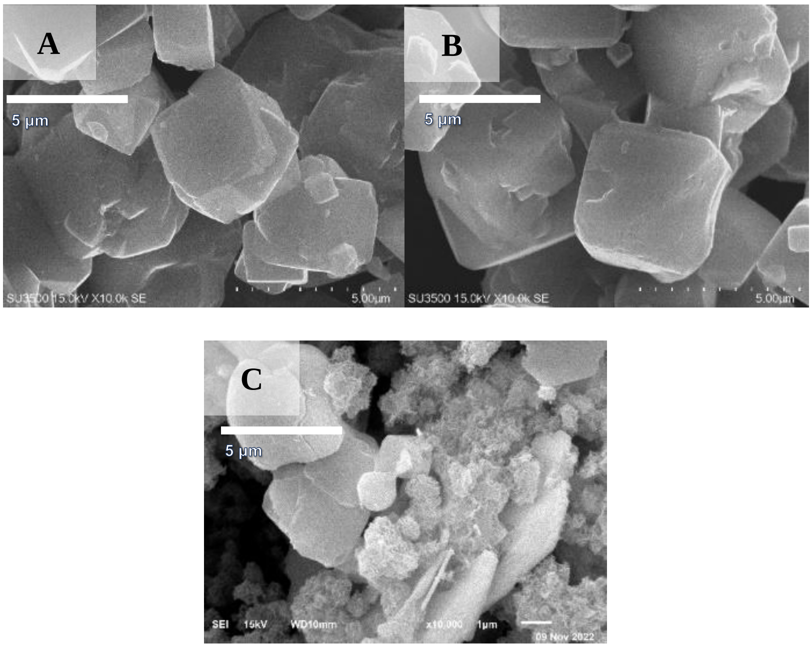

Figure 3 Morphology of zeolite A (A), zeolite-NaOH (B), and zeolite-$CaCO_3$ (C)

3.2 Crystallography

The diffractogram of all three samples are shown in Figure 4 and Figure 5. Diffractogram of zeolite A shows that it had an extremely high crystallinity, indicated by sharp peaks and almost no amorphous phase. Treatment using NaOH did not change this reading, which further confirms the lack of morphological changes caused by it.

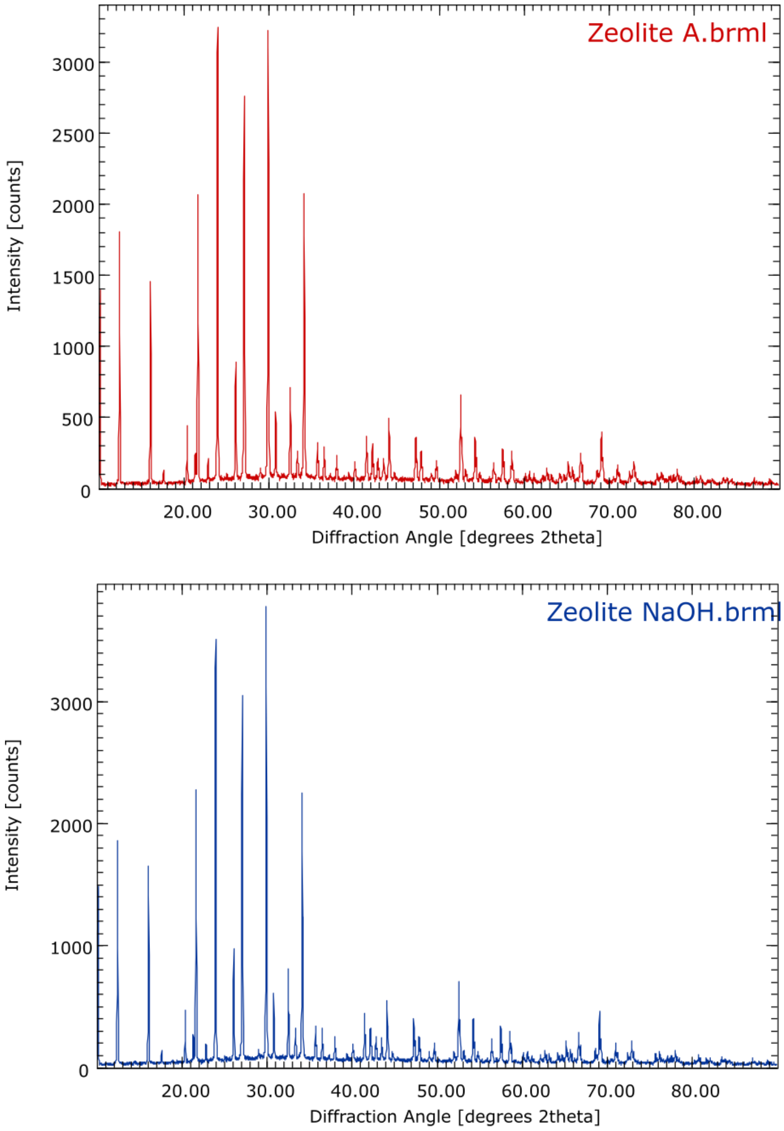

Figure 4 Diffractogram of zeolite A and zeolite-NaOH

Addition of $CaCO_3$ as shown in Figure 5 causes the formation of amorphous phases, mainly at 2θ position ~25° to 35°, and the appearance of CaO, $Ca(OH)_2$ and $CaCO_3$ characteristic peaks. The peaks of zeolite A are otherwise unchanged. The presence of significant $Ca(OH)_2$ peaks is unexpected. Previous measurements (using pure $Ca(OH)_2$ decomposed in TGA by Mirghiasi *et al.* [13]) shows that decomposition of $Ca(OH)_2$ happens at temperatures ranging from 380 to 475°C, so this reading most likely means that the water evaporated during calcination was somehow reincorporated into the material after calcination.

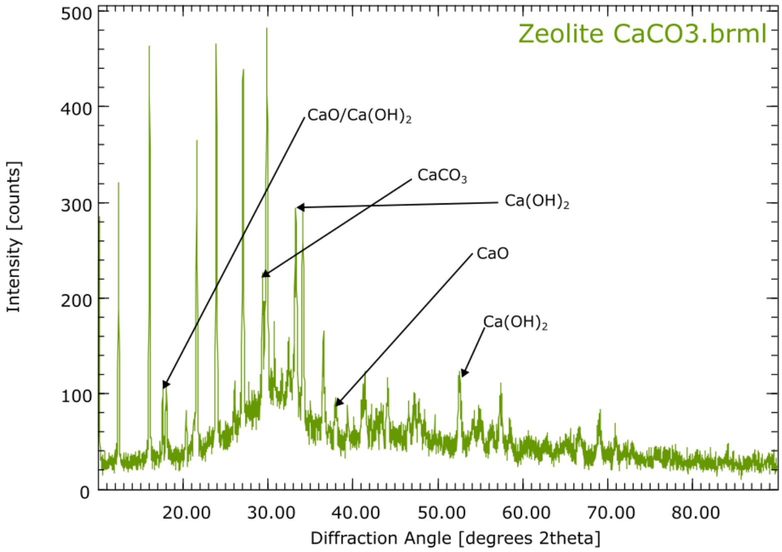

Figure 5 Diffractogram of zeolite-$CaCO_3$. Peak information is from ICDD (Gates-Rector and Blanton [14])

3.3 Thermogravimetry

The thermogravimetric curve and temperature of the samples are given in Figure 6.

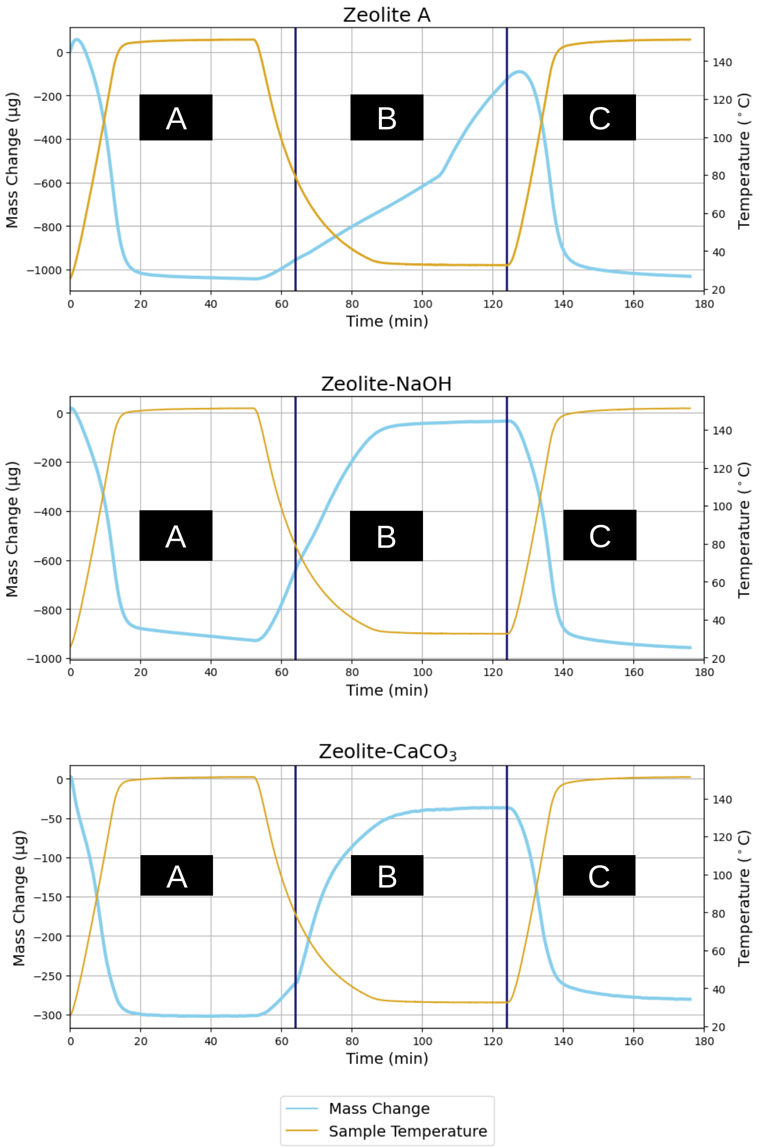

Figure 6 Thermogravimetric and temperature plot of zeolite A, zeolite-NaOH, and zeolite-$CaCO_3$

The plot shows that zeolite A could adsorb up to roughly 12% of its mass in CO_2. However, this adsorption occurs relatively slowly, with the curve not peaking even after 1 h of continuous adsorption. Addition of NaOH fixed this problem. Unfortunately, a significant amount of N_2 was absorbed, thus reducing the adsorption capacity of zeolite-NaOH, and showing that zeolite-NaOH had significant selectivity problem. Meanwhile, it was observed that zeolite-$CaCO_3$ demonstrated an apparent decrease of adsorption capacity. However, upon considering the proportion of zeolite in zeolite-$CaCO_3$, it could be shown that the adsorption capacity of the material actually increases. $CaCO_3$ presence also fixed the selectivity problem, as shown by the reduction of N_2 adsorbed by zeolite-$CaCO_3$ compared to zeolite-NaOH.

By looking at the TG plot in step C, it could be determined that all samples could effectively desorb CO_2 at relatively similar speeds. By the end of step C, the TG curve position is effectively the same between zeolite A and zeolite-NaOH. In contrast, the TG curve position in step C is slightly higher. This is due to conversion of CaO to $CaCO_3$ in zeolite-$CaCO_3$. The slight change shows that the proportion of CaO is relatively minimal.

To account for the zeolite proportion of zeolite-$CaCO_3$, the proportion of the calcium species in the samples must be considered. XRD diffractogram in Figure 5 shows that in addition to the crystalline phase of CaO, Ca(OH), and $CaCO_3$, significant amorphous phase was also found in zeolite-$CaCO_3$. Determining the composition of samples containing multiple compounds is not straightforward, as it cannot be simply deduced from the number or intensity of the peaks in the diffractogram. Additionally, the presence of a significant amorphous phase further complicates the analysis. Therefore, in order to account for the proportion of zeolite in such samples, certain assumptions need to be taken. To simplify things, three assumptions are made in this paper : all $Ca(OH)_2$ was converted to $CaCO_3$ (assumption 1), half converted to $CaCO_3$ (assumption 2), or not converted to $CaCO_3$ (assumption 3). The first assumption means that the mass proportion between zeolites and calcium species changes to 1:1.03, while the second means that the mass proportion became 1:0.9, and the last means that the mass proportion stays at 1:0.77. The change in mass proportion is due to the increase of molar mass ($Ca(OH)_2$ molar mass is 74 gr/mol, while $CaCO_3$ molar mass is 100 gr/mol).

Calculated adsorption capacity $\left(C_{\mathrm{CO_2}}\right)$ values of the materials are given in Table 1. $C_{\mathrm{CO_2}}$ is calculated by dividing the ‘Step B mass difference’ column with ‘Sample Mass’ column. It is also converted to molar units by dividing it with molar mass of CO_2 (44 g/mol).

Significant differences in sample mass are due to the nature of sample loading in the TG/DTA machine, which accounts for volume (the sample must fill a determined volume in the crucible).

Table 1 Calculated adsorption capacity $\left(C_{\mathrm{CO_2}}\right)$ of the materials

No	**Sample**	**Sample mass (mg)**	**Step B mass difference (μg)**	**$C_{\mathrm{CO_2}}$ (mg CO_2 per g adsorbent)**	**$C_{\mathrm{CO_2}}$ (mmol CO_2 per g adsorbent)**
1	Zeolite A	6.722	828.361	123.231	2.8
2	Zeolite-NaOH	5.645	607.165	107.558	2.4
3	Zeolite-$CaCO_3$ (apparent)	2.982	223.488	74.946	1.7
4	Zeolite-$CaCO_3$ (Assumption 1)	1.467	223.488	152.316	3.4
5	Zeolite-$CaCO_3$ (Assumption 2)	1.569	223.488	142.397	3.2
6	Zeolite-$CaCO_3$ (Assumption 3)	1.684	223.488	132.654	3.0

Data from Table 1 shows that untreated zeolite A had an adsorption capacity of 2.8 mmol CO_2 per g adsorbent (also written as mmol/g). Due to significant adsorption of N_2 as shown in Figure 6, the adsorption capacity of zeolite-NaOH is reduced to 2.4 mmol/g. Apparent adsorption capacity of zeolite-$CaCO_3$ is further reduced to 1.7 mmol/g. This is due to the presence of a significant amount of nonadsorbing calcium species (CaO, $CaCO_3$, $Ca(OH)_2$). However, by calculating the amount of zeolite in zeolite-$CaCO_3$ and computing the adsorption capacity using it, it could be shown that the adsorption capacity of zeolite A actually increases, even in assumption C where it was assumed that all $Ca(OH)_2$ was unconverted.

The adsorption kinetics (v) of the material is presented in Table 2. To obtain v, the sample mass at the 74th minute was subtracted by the sample mass at the 64th minute, then divided by 10. To account for differences in mass, comparison between materials is done by converting the adsorption kinetics unit from μg per minute to mg CO2 per gram adsorbent per minute (also called mgg/min). This conversion is done by dividing it with sample mass.

Table 2 Adsorption kinetics (v) of the materials

No	Sample	Sample mass (mg)	Sample mass		v (µg/min)	v (mgg/min)
			64th min (A)	74th min (B)		
1	Zeolite A	6.722	-954.953	-861.289	9.366	1.393
2	Zeolite-NaOH	5.645	-640.225	-351.543	28.86	5.113
3	Zeolite-$CaCO_3$ (apparent)	2.982	-260.006	-124.274	13.573	4,552
4	Zeolite-$CaCO_3$ (Assumption 1)	1.467	-260.006	-124.274	13.573	9.239
5	Zeolite-$CaCO_3$ (Assumption 2)	1.569	-260.006	-124.274	13.573	8.648
6	Zeolite-$CaCO_3$ (Assumption 3)	1.684	-260.006	-124.274	13.573	8.056

Table 2 showed that the adsorption kinetics of zeolite improved massively by addition of NaOH, shown by the increase of v from 1.393 mgg/min to 5.113 mgg/min. The presence of $CaCO_3$ leads to a deceleration in adsorption to 4.552 mgg/min, which is still four times faster than untreated zeolite A. However, by accounting for zeolite mass only, the adsorption process actually happens even faster, with even the slowest assumption at 8.056 mgg/min, about 60% faster than zeolite-NaOH and eight times faster than raw zeolite A.

N_2 adsorption $\left(C_{\mathrm{N}_2}\right)$ of the materials is given in Table 3, To obtain C_{N_2}, the 'B-A' column is divided with 'Sample mass' column.

Table 3 N_2 adsorption $\left(C_{\mathrm{N_2}}\right)$ of the materials

No	Sample	Sample mass (mg)	Minimum mass difference in Step A (µg) (A)	Mass difference at the beginning of Step B (µg) (B)	B-A (µg)	$C_{\mathrm{N_2}}$ (mg N_2 per g adsorbent)
1	Zeolite A	6.722	-1043.191	-954.953	88.238	13.127
2	Zeolite-NaOH	5.645	-928.789	-640.225	288.564	51.119
3	Zeolite-$CaCO_3$ (apparent)	2.982	-302.425	-260.006	42.419	14.225
4	Zeolite-$CaCO_3$ (Assumption 1)	1.467	-302.425	-260.006	42.419	28.915
5	Zeolite-$CaCO_3$ (Assumption 2)	1.569	-302.425	-260.006	42.419	27.028
6	Zeolite-$CaCO_3$ (Assumption 3)	1.684	-302.425	-260.006	42.419	25.178

Data presented in Table 3 shows that zeolite A exhibits significant selectivity towards N_2 with minimal adsorption occurring. Treatment with NaOH significantly reduces its selectivity, with N_2 adsorption in zeolite-NaOH increasing by approximately four times compared to untreated zeolite A. Incorporation of $CaCO_3$ resolves this issue, with zeolite-$CaCO_3$ had N_2 adsorption only slightly higher than untreated zeolite A (if considering total) or twice as high (if only taking zeolite into account, for all assumptions).

4 Conclusion and Future Work

In conclusion, the presence of $CaCO_3$ improves the adsorption capacity, kinetics, and selectivity of zeolite A. While treatment with NaOH is sufficient to improve the adsorption kinetics of zeolite A, it comes at the cost of reducing its selectivity, seen by the adsorption of significant amounts of N_2. The presence of $CaCO_3$ mitigates that problem.

In this research, $CaCO_3$ was accompanied by CaO and $Ca(OH)_2$ in intercalating with zeolite A. The presence of CaO is somewhat expected due to incomplete carbonation to $CaCO_3$, while the presence of $Ca(OH)_2$ is unexpected. However, the presence of $Ca(OH)_2$ theoretically could improve the binding of CO_2 due to its alkaline nature. Further research is needed to determine the usability of $Ca(OH)_2$ as activation agents. While CaO readily reacts with CO_2 and forming

$CaCO_3$, this reaction is only reversible in calcination temperatures (600-750°C), and thus is inapplicable for this research.

Furthermore, exploration of methods that do not involve calcination is also desirable. While calcination is useful for activating zeolite, it is also very energy intensive. One method that does not involve calcination in synthetizing $CaCO_3$ is by reacting calcium hydroxide with natrium carbonate. Further research is needed to determine whether that method gave similar, or even better, results than this research.

Finally, further research may investigate varying ratios of calcium species to zeolite A to minimize the reduction in the apparent adsorption capacity of zeolite-$CaCO_3$.

5 Nomenclature

$C_{\mathrm{CO_2}}$ = Carbon dioxide adsorption capacity of the adsorbents

$C_{\mathrm{N_2}}$ = Nitrogen adsorption of the adsorbents

v = Adsorption kinetics

Acknowledgements

Research done in this paper is funded by eASIA-JRP Program Year 2022.

References

[1] E. Rubin, J. C. Abanades, M. Akai, S. Benson, D. Keith, M. Mazzotti, B. Metz, B. Osman-Elasha, A. Palmer, K. Smekens, and M. Soltanieh, *IPCC Special Report : Carbon Dioxide Capture and Storage*, 1st ed. New York, USA: Cambridge University Press, 2005.

[2] S. Bajpai, N. Shreyash, S. Singh, A. R. Memon, M. Sonker, S. K. Tiwary, and S. Biswas, “Opportunities, challenges and the way ahead for carbon capture, utilization and sequestration (CCUS) by the hydrocarbon industry: Towards a sustainable future,” *Energy Reports*, **8**, pp. 15595–15616, Nov. 2022, doi: 10.1016/j.egyr.2022.11.023.

[3] F. Raganati, F. Miccio, and P. Ammendola, “Adsorption of Carbon Dioxide for Post-Combustion Capture: A Review,” *Energy Fuels*, **35**(16), pp. 12845–12868, Aug. 2021, doi: 10.1021/acs.energyfuels.1c01618.

[4] M. Younas, M. Sohail, L. K. Leong, M. J. Bashir, and S. Sumathi, “Feasibility of CO2 adsorption by solid adsorbents: a review on low-

temperature systems," *Int. J. Environ. Sci. Technol.*, **13**(7), pp. 1839–1860, Jul. 2016, doi: 10.1007/s13762-016-1008-1.

[1] W. Lutz, "Zeolite Y: Synthesis, Modification, and Properties—A Case Revisited," *Advances in Materials Science and Engineering*, vol. 2014, pp. 1–20, 2014, doi: 10.1155/2014/724248.

[2] V. Indira and K. Abhitha, "A review on recent developments in Zeolite A synthesis for improved carbon dioxide capture: Implications for the water-energy nexus," *Energy Nexus*, **7**, p. 100095, Sep. 2022, doi: 10.1016/j.nexus.2022.100095.

[3] O. Cheung, Z. Bacsik, Q. Liu, A. Mace, and N. Hedin, "Adsorption kinetics for CO2 on highly selective zeolites NaKA and nano-NaKA," *Applied Energy*, vol. 112, pp. 1326–1336, Dec. 2013, doi: 10.1016/j.apenergy.2013.01.017.

[4] A. Gao, N. Guo, M. Yan, M. Li, F. Wang, and R. Yang, "Hierarchical porous carbon activated by CaCO3 from pigskin collagen for CO2 and H2 adsorption," *Microporous and Mesoporous Materials*, v**260**, pp. 172–179, Apr. 2018, doi: 10.1016/j.micromeso.2017.08.048.

[5] Y. Areerob, D. C. T. Nguyen, B. M. R. Dowla, H. Kim, J.-W. Cha, and W.-C. Oh, "Synthesis and Characterization of Calcium Derivative Combined with High-Surface-Area Activated Carbon Composites for Fine Toxic Gas Removal," *J. Korean Ceram. Soc*, **55**(5), pp. 473–479, Sep. 2018, doi: 10.4191/kcers.2018.55.5.02.

[6] E. E. Khine, D. Koncz-Horvath, F. Kristaly, T. Ferenczi, G. Karacs, P. Baumli, and G. Kaptay, "Synthesis and characterization of calcium oxide nanoparticles for CO2 capture," *J Nanopart Res*, **24**(7), p. 139, Jul. 2022, doi: 10.1007/s11051-022-05518-z.

[7] Y.-H. Chen and D.-L. Lu, "CO2 capture by kaolinite and its adsorption mechanism," *Applied Clay Science*, **104**, pp. 221–228, Feb. 2015, doi: 10.1016/j.clay.2014.11.036.

[8] S. Thakur, S. Singh, and B. Pal, "Time-dependent growth of CaO nano flowers from egg shells exhibit improved adsorption and catalytic activity," *Advanced Powder Technology*, **32**(9), pp. 3288–3296, Sep. 2021, doi: 10.1016/j.apt.2021.07.015.

[9] Z. Mirghiasi, F. Bakhtiari, E. Darezereshki, and E. Esmaeilzadeh, "Preparation and characterization of CaO nanoparticles from Ca(OH)2 by direct thermal decomposition method," *Journal of Industrial and Engineering Chemistry*, **20**(1), pp. 113–117, Jan. 2014, doi: 10.1016/j.jiec.2013.04.018.

[10] S. Gates-Rector and T. Blanton, "The Powder Diffraction File: a quality materials characterization database," *Powder Diffr.*, **34**(4), pp. 352–360, Dec. 2019, doi: 10.1017/S0885715619000812.